International Journal of Nanoelectronics and Materials
Volume 13 (Special Issue) May 2020 [285-294]

External Patch Fillet Repair for Sulphur Recovery Unit of Petroleum Refinery Plant

Abdul Razak Abdul Rahman[1], Fudhail Abdul Munir[2,3]*, Eddy Azrai Ariffin[1], Nurfarah Diana Ridzuan Tan[2,3] and Herman Saputro[4]

[1]*Malaysian Refining Company Sdn Bhd, Persiaran Penapisan, Sungai Udang, Melaka, Malaysia.*
[2]*Centre of Advanced Research on Energy (CARe) Universiti Teknikal Malaysia Melaka, Hang Tuah Jaya Durian Tunggal, Melaka, Malaysia.*
[3]*Faculty of Mechanical Engineering, Universiti Teknikal Malaysia Melaka, Hang Tuah Jaya Durian Tungga, Melaka, Malaysia.*
[4]*Department of Mechanical Engineering Education, Sebelas Maret University, Jl. Ahmad Yani No.200, Pabelan, Surakarta, Indonesia.*

ABSTRACT

The main function of Sulphur Recovery Unit (SRU) is to recover 99.2% of sulphur from the feed of Amine Regeneration Unit (ARU) and Sour Water Treating Unit (SWTU). Hotspot related problem or localized burning can be detrimental to the SRU material lifespan. One of the causes of the hotspot is susceptible high vibration level of multi-components in SRU. Downing of SRU in any refinery plant leads to unplanned losses in revenue. Thus, thorough routine maintenance needs to be performed to avoid such disruption. In this project, the method of repairing part of the SRU reheater external wall is presented. External patch fillet is introduced to seal the damaged reheater external shell wall. Before the maintaining process, the root cause of the problem is first examined. Fitness for service (FFS) is also performed to ensure that the repair method is sufficient for continuous operation. The obtained results from the assessments were used to conduct the required repair services. All assessment and repair methods are based on the guidelines set by the relevant codes and standards.

Keywords: Sulphur Recovery Unit (SRU), Localized Burning, Fitness for Service (FFS).

1. INTRODUCTION

In the oil refining process, there are various methods developed to remove unwanted acidic gases. Hydrogen sulphide (H_2S) and carbon dioxide (CO_2) are examples of these acid gases that are generated in large quantities from the desulphurization of natural gas [1]. Meanwhile, small quantities of impurities such as N_2, NH_3, CS_2, COS and hydrocarbons are also derived from these gases [2, 3]. H_2S and CO_2 can be converted into syngas to remove these acidic gases. The element of sulphur from these acid gases can be recovered by various methods such as direct oxidation, Unisulf, Takahax, Selectox and Claus process [4]. Claus process generally is the most popular method to maximize the elemental sulphur production from acid gases.

Sulphur Recovery Unit (SRU) is commonly utilized in the relevant oil and gas industry to process acid gases in the natural gas processing units [1]. The acidic gas which is hydrogen sulphide is mitigated to the SRU to produce elemental sulphur [5]. The main components of SRU are a burner, a reaction furnace, a waste heat boiler (WHB) and a train of sulphur condensers. In SRU, the stream of acidic gases at specified pressure is supplied to the reaction furnace burner together with the correct ratio of air [6]. Combustion in SRU can be well simulated using commercial Computational Fluid Dynamics (CFD) software. Optimization of SRU can be made with such

*Corresponding Author: *fudhail@utem.edu.my*

simulations results. However, simulations results cannot be the sole factor for any enhancement [7]. The function of this stream of air is to oxidize the feed of contaminates.

Then, the acidic gases will be combusted at temperatures ranging from 975 to 1300°C in the reaction furnace. Generally, the SRU process involves thermal reactor furnace that is called a thermal stage. Meanwhile, the SRU process that involves Claus reheater and SuperClaus reheater is called catalytic stage [8]. The sulphur is condensed and collected between stages of condensers before it is delivered to sulphur pits. The reheater reheats the process gas to an optimum temperature to achieve a high conversion of H_2S and SO_2 to elementary sulphur. The condenser is used to condense sulphur vapour into liquid sulphur and is drained to the sulphur pit. Unrecovered sulphur exits the plant through the tail gas incinerator in the form of SO_2.

In this project, the method of repairing the SRU wall due to thinning is presented. Routine inspection detected irregularities on the part of the SRU reheater external shell wall. In order to avoid future unplanned operation disruption, the repair was performed according to codes and standards.

2. MATERIAL AND METHODS

2.1 Root Cause Investigation

The SuperClauss (RC) Reheater was found with a localized burning mark in the insulation cladding, rockwool and shell wall. The damaged mark is illustrated in Figure 1. The shell wall found with dark colour, which is suspected due to the internal localized fire. It is a well-known fact that for any fire ignition to occur, the critical three elements that must be simultaneously present are fuel, oxygen and ignition [9]. Generally, the localized burning in process equipment is mostly due to the presence of pyrophoric iron sulphide in the sour gas refinery process [10-12]. Pyrophoric iron sulphide is formed by the reaction of hydrogen sulphide (>1%) with the rust of carbon steel. The reaction between the two materials forms an iron rust scale on the metal surface. Pyrophoric iron can instantaneously ignite when exposed to air. Therefore, localized burning due to pyrophoric is not uncommon in the sulphur recovery process. The exothermic reaction of pyrophoric iron with air releases a tremendous amount of heat. The amount of heat is enough to make the iron deposits to glow and turns red in colour. Apart from that, the high heat created is adequate to ignite any fuel source and consequently causes fires. The following is the exothermic reaction between iron sulphides that is in contact with air, which can create a high amount of heat:

$$4FeS + 7O_2 = 2Fe_2O_3 + 4SO_2 + heat \quad (1)$$

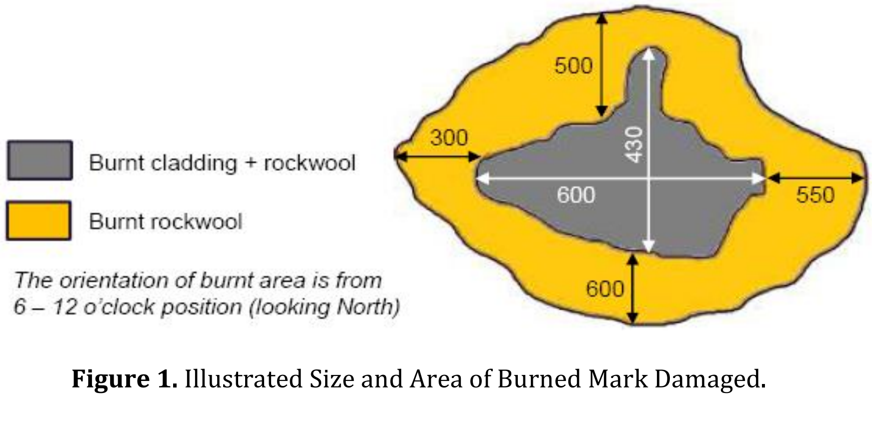

Figure 1. Illustrated Size and Area of Burned Mark Damaged.

The burning also leads to high temperature corrosion damage that is called sulphidation to equipment and piping resulting in higher corrosion rate than the usual experienced due to the formation of H_2SO_4. Sulphidation is defined as corrosion of carbon steel resulting from their reaction with sulphur compounds in high temperature environments. Furthermore, the presence of hydrogen accelerates corrosion. Sulphur blockage at a 6-inch diameter of air purge line was found during a previous routine inspection. The air purge line is a carbon steel insulated pipe, however, the line is not well insulated due to damaged rockwool insulation. Carbon steel piping is highly susceptible to the formation of pyrophoric iron sulphide. The presence of sulphur blockage suggests that there is insufficient heating causing sulphur to accumulate. Apart from that, the temperature must be above 138°C to prevent an acid dew point corrosion (ADPC). The aim of the design is to pre-heat the purge air before entering SuperClaus process stream to prevent ADPC.

2.2 Integrity Assessment Fitness for Service (FFS)

Upon the confirmation of the issue, integrity of the equipment is made as per API 579 (Fire Damage to Carbon and Low Alloy Steels (Fire case)). The following assessments were carried out to evaluate the equipment integrity after the incident:

i. Replica Test
ii. Hardness Check
iii. Thickness Check

2.3 Maintenance Work

The repair is undertaken in accordance with API 510 [13] which also refers to ASME PCC-2 (Repair of Pressure Equipment and Piping [14]. One of the repair options for the damaged due to localized wall thinning is by applying an external patch plate on the damaged area. The design approach for this repair method is based on the standard pressure component design calculation, as per ASME BPVC Section VIII Division 1 [15]. The requirements as mentioned in [13] are as follows:

i. The application limitation imposed apply to the governing loads resulting from internal working pressure where the resultant stress is membrane stress.
ii. The material of plate shall be same or very similar to the base material of the component, which taking consideration the mechanical properties and compatibility of the material with the process medium and operating parameters (pressure and temperature).
iii. The thickness of the patch plate is dependent on material mechanical properties and attachment weld sizes.
iv. The size of the patch plate (length and wide) is governed by the requirement that all welds attachment (patch plate) completely cover the damaged areas.
v. The weld attachment distance from the sound base metal should be at least 25 mm.
vi. The edge corner must be fabricated with a minimum radius of 75 mm (3 inches). If weld on top the existing seam weld is unavoidable, it should be ground flush with the vessel outside diameter and examined by the Magnetic Particle Test (MPT) or Dye Penetrant Test (DPT).

3. RESULTS AND DISCUSSION

3.1 Material Characteristics

3.1.1 Surface Replica of Heated Area

Replica assessment is to identify grain growth measurement (ASTM E112) of the affected area. Six (6) replicated location on the shell wall were taken and evaluated. Three (3) points of the unburned location were located and compared with three (3) points of burned location. The surface replica testing result is categorized as Rating 1 as indicated in Table 1. It was identified that there is a coarser grain at the burned location instead of fine grain as depicted in Figure 2. There is 41% grain growth, indicating steel was likely exposed to above A3 temperature (>930°C) and slow cooling. If the material is exposed to a temperature between 1030°C to 1095°C, then the grain size increased dramatically. The grain growth is a sign of a reduction in strength of the material that might cause the equipment to fail if the similar incident reoccurs.

Table 1 Grain size at six (6) replicated location

Replicated Location	Grain Size			
	1	2	3	Avg
Burn 1	5.34	4.71	5.18	5.08
Burn 2	5.06	4.60	5.02	4.89
Burn 3	4.42	4.89	4.39	4.57
Unburn 1	7.30	6.72	6.84	6.95
Unburn 2	7.69	7.74	7.91	7.78
Unburn 3	7.89	7.67	7.62	7.73

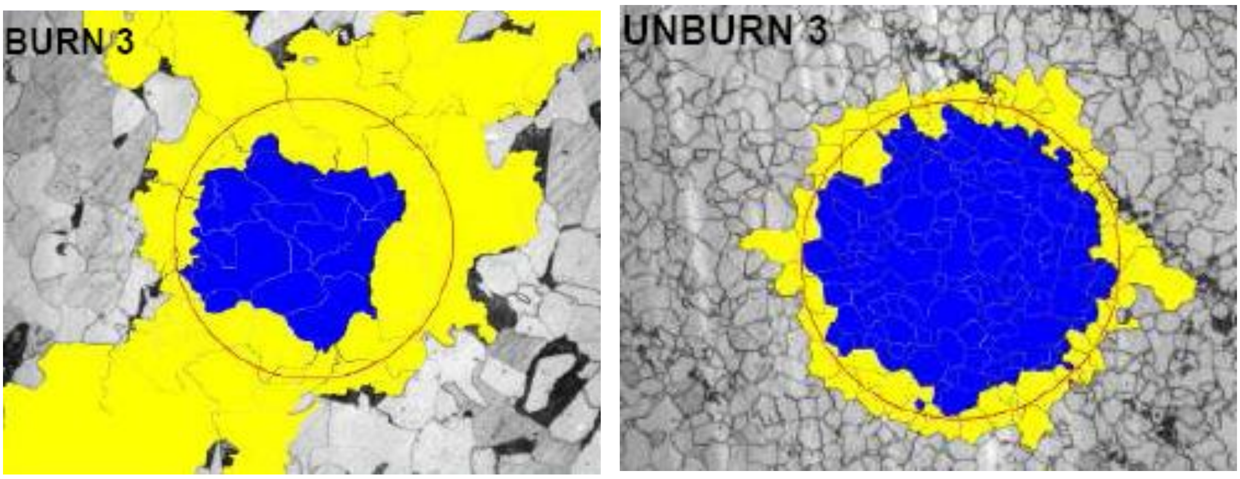

Figure 2. Microstructure grain growth at Location 3.

3.1.2 Material Hardness Check

Material hardness check was performed to obtain the data needed for a metallurgical review. The result of hardness performed is within an acceptable range. Based on the hardness values obtained after the incident, the material is categorized as acceptable. The hardness value result is between 126 to 171 HV, which is within the acceptable limit of hardness value 100 to 220 HV for a material A 516 Gr 60 at the design temperature of 270°C. Therefore, the material passes the FFS 579 Level 1 metallurgical assessment.

3.1.3 Shell Wall Thickness Check

It is observed that the area is affected by severe corrosion damage, which is due to the high temperature of sulfidation. The thickness is reduced from 14.00 mm to 3.19 mm in the localized area identified from the Ultrasonic Thickness Measurement (UTM) results. The grid was established on the affected area. This corrosion rates can be considered as a very high localized corrosion rate for a carbon steel type of shell wall.

3.2 Calculated Internal Pressure Load

The required repair surface is a shell with a cylindrical shape. Hence, the plate is subjected to internal pressure load, which are in circumferential and longitudinal component load. The circumferential load calculation is given in Equation (2) and Figure 3.

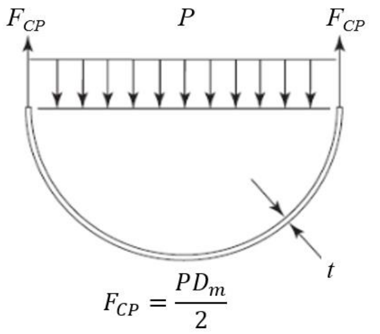

Figure 3. Illustration of a plate subjected to internal pressure.

$$F_{CP} = \frac{PD_m}{2} \tag{2}$$

where,

D_m = diameter at the mid-wall component, mm
F_{CP} = circumferential force due to internal pressure, N/mm
P = internal design pressure, kPa

Knowing that the internal design pressure is set to 353 kPA while the diameter at mid-wall of component is 1000 mm. Thus, the calculated total circumferential force from all loads is 176520 N/mm. Meanwhile, the calculated longitudinal force to the internal pressure is 88259.8 N/mm. The method of calculating the longitudinal force is as in Equation (3) and the direction of the relevant forces is depicted in Figure 4.

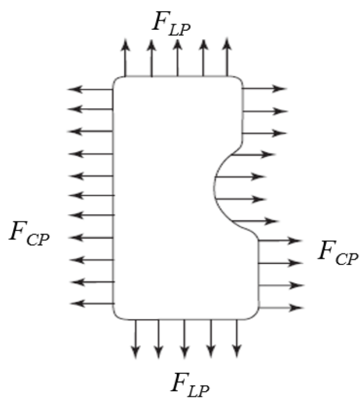

Figure 4. Illustration of a plate subjected to internal pressure.

$$F_{LP} = \frac{PD_m}{4} \quad (3)$$

where,

F_{LP} = longitudinal force due to internal pressure N/mm

If other loads are applicable (such as bending, torsion, wind) they shall be determined and added to the pressure load such that:

$$F_C = F_{CP} + F_{CO} \text{ and } F_L = F_{LP} + F_{LO} \quad (4)$$

where,

F_C = the total circumferential force from all loads, N/mm
F_{CO} = circumferential force due to other applicable loads, N/mm
F_L = the total longitudinal force from all loads, N/mm
F_{LO} = longitudinal force due to other applicable loads, N/mm

3.3 Calculation of allowable load on the perimeter fillet weld

The perimeter weld shall be sized as such that the allowable load on the weld exceeds the longitudinal and circumferential loads as calculated in section 3.2. The weld thickness size shall not exceed the thickness of material joined nor 40 mm. The plate edge preparation may be bevelled to increase the weld's effective throat thickness.

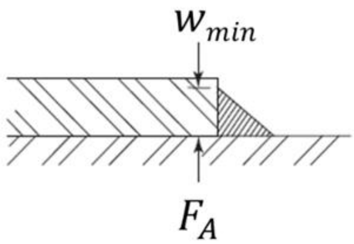

$$F_A = w_{min} E S_a \quad (5)$$

where.

E = weld joint efficiency factor (0.55)
F_A = allowable force on fillet welds, N/mm; $F_A > F_C$ and F_L
S_a = allowable base metal stress, MPa
w_{min} = minimum weld leg dimension, mm

The calculated allowable force on the fillet weld (F_A) is 1056440 N/mm, which is significantly larger than the total circumferential and longitudinal of all load (determined in section 3.2).

3.4 Site work

The site work involves the preparation of the patch plate to the required shape dimension. The method can be mechanical or thermal cut that is either flame or arc cutting. If it is by thermal cutting, a minimum of 1.5 mm additional material shall be removed by grinding or machining. It is to eliminate any parent metal degradation or defect which lead to weld failure during the fitting process and operation. Since the plate thickness used is 15.9 mm which is less than 25 mm, the fillet weld leg should be less than 15.9 mm. The patch plate as shown in Figure 5 must be fitted as tight as possible to the surface to be welded and shall not have more than 5 mm separation between the two faces. If the separation at facing edge is 1.5 mm or greater, the separation value must be added to the eccentricity and the weld parameter should be re-calculated.

The surface area to be welded must be cleared from rust, paint, scale and liquids or other foreign material that could produce lamination or weld defect inclusion of tungsten or porosity. The area of weld zone with a minimum of 40 mm must be cleaned on both sides of the weldment before welding. The fillet patch location is depicted in Figure 6.

Figure 5. Patch plate utilized for the patch fillet.

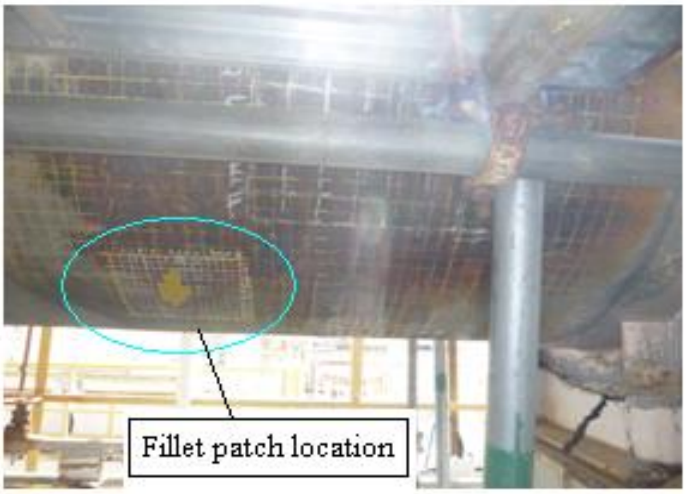

Figure 6. Patch fillet location.

After the surface preparation on the affected area, Magnetic Particle Testing (MPT) was performed to ensure the surface is free from any defect or leakage. Dehydrogenation on the working surface at 250°C for 2 hours was performed before fit up after completion of surface preparation and examination tests. Since this equipment is exposed to liquid H_2S environment, heating pad with insulation is used to avoid hydrogen blistering during welding.

The patch plate was then fitted up onto the shell wall and it was observed for any separation between plate and shell. The measured maximum separation distance is 5 mm which is acceptable by the standard. Once this critical criterion is satisfied, the plate is then welded on the shell using the welding sequence as shown in Figure 7 to minimize plate distortion. To avoid gas pressure build-up between the patch plate and the pressure component boundary, provisions for venting during the final closure weld or post-weld heat treatment is necessary.

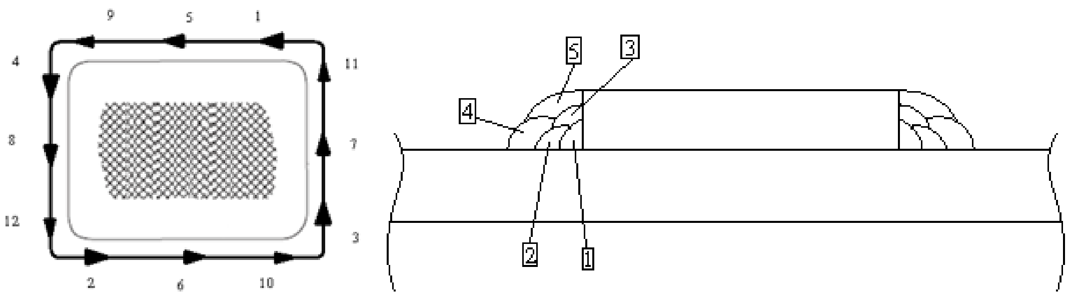

Figure 7. Welding sequence.

Magnetic Particle Testing (MPT) (root and capping) and hardness testing shall be performed after welding completed by a certified welding inspector to ensure free from any defect (max hardness value for carbon steel 225 HBW). Figure 8 depicts the location of the hardness point. For the final acceptance, the hydro test was performed at the shell side. Shell side test pressure was set at 5.4 kg/cm2. The baseline thickness of the patch plate was measured using UT grid scanning. Finally, the patched area was cleaned and painted as per the Petronas Technical Standard (PTS) 15.20.03 was applied (coating system M-9-3).

Figure 8. Location for Hardness Test after Fillet Weld.

4. CONCLUSION

The crucial method of repairing the SRU reheater external wall is successfully presented. The repair process should strictly follow the code and engineering standards set by the Americal Society of Mechanical Engineers (ASME) and internal company policies. Acid Dew Point corrosion (ADPC) occurs due to the hydrocarbon carried over, sulphur accumulation and insufficient heating of acid gas. This phenomenon results from iron sulphide or pyrophoric iron ignition, which when combines with excess air from the purge air can lead to the localized burning. The appropriate attention on maintaining heating insulation for critical equipment should be put in place. It also appropriates to conduct a site survey at the SRU plant to identify the piping and equipment with inadequate or damaged heating insulation.

The pyrophoric iron formation is the most susceptible defect that occurs on piping and equipment carbon steel piping. Purge air piping which is made from carbon steel should be upgraded to material that has resistance towards pyrophoric iron formation like SelOX air pipe. The evident grain growth for the shell wall material is the sign of a reduction in strength of the material that may cause the equipment to fail should the incident re-occurs. Therefore, a permanent repair to replace the shell area by inserting a patch method is required during the plant shutdown to avoid further risk.

ACKNOWLEDGEMENT

The authors gratefully acknowledge the support by Malaysian Refining Company Sdn Bhd (MRCSB) and Universiti Teknikal Malaysia Melaka (UTeM). This research is partly sponsored by an industrial grant with the number AMIC/2019/FKM-CARE.

REFERENCES

[1] Mahmoodi B, Hosseini SH, Ahmadi G, Raj A. CFD simulation of reactor furnace of sulfur recovery units by considering kinetics of acid gas (H2S and CO2) destruction. Applied Thermal Engineering **123** (2017) 699-710.

[2] Ibrahim S, Raj A. Kinetic Simulation of Acid Gas (H2S and CO2) Destruction for Simultaneous Syngas and Sulfur Recovery. Industrial & Engineering Chemistry Research **55** (2016) 6743-52.

[3] Rahman ARA, Ariffin EA, Abu MH, Munir FA, Putra A. Experimental Investigation of Thermally Induced Vibration in Sulphur Recovery Unit (SRU). Journal of Advanced Research in Fluid Mechanics and Thermal Sciences **56** (2019) 78-87.

[4] Cover AE, Hubbard DA, Jain SK, Shah KV, Koneru PB, Wong EW. Review of Selected Sulfur Recovery Processes for SNG production. Gas Research Institute, (1985).

[5] Lins VFC, Guimarães EM. Failure of a heat exchanger generated by an excess of SO2 and H2S in the Sulfur Recovery Unit of a petroleum refinery. Journal of Loss Prevention in the Process Industries **20** (2007) 91-97.

[6] Wagenfeld J-G, Ali KA, Almheiri S, Slavens AF. Sustainable applications utilizing sulfur, a by-product from oil and gas industry: A state-of-the-art review. Waste Management **98** (2019) 78-89.

[7] Fudhail AM, Sidik NAC, Rody MZM, Zahir HM, Musthafah MT. Numerical Simulations of Shear Driven Square and Triangular Cavity by Using Lattice Boltzmann Scheme. World Academy of Science, Engineering and Technology **45** (2010) 190-194.

[8] A. GA, A. S, Sh. M. Maximization of sulfur recovery efficiency via coupled modification of GTU and SRU processes. Egyptian Journal of Petroleum **26** (2017) 579-592.

[9] Munir FA, Zainuddin MIM, Gader A, Mikami M, Saputro H, Fitriana L. Effects of Wall Thickness on Flame Stabilization Limits for Combustors with Wire Mesh. Journal of Advanced Research in Fluid Mechanics and Thermal Sciences **49** (2019) 11-17.

[10] Bertolini M, Bevilacqua M, Ciarapica FE, Giacchetta G. Development of Risk-Based Inspection and Maintenance procedures for an oil refinery. Journal of Loss Prevention in the Process Industries **22** (2009) 244-253.

[11] Manenti G, Papasidero D, Manenti F, Bozzano G, Pierucci S. Design of SRU Thermal Reactor and Waste Heat Boiler Considering Recombination Reactions. Procedia Engineering **42** (2012) 376-383.

[12] Manenti F, Papasidero D, Bozzano G, Ranzi E. Model-based optimization of sulfur recovery units. Computers & Chemical Engineering, 66 (2014). 244-251.
[13] API. Pressure Vessel Inspection Code: Maintenance Inspection, Rating, Repair, and Alteration. American Petroleum Institute, (1997).
[14] ASME. Repair of Pressure Equipment and Piping. New York: The American Society of Mechanical Engineers, (2011).
[15] ASME. ASME Boiler & Pressure Vessel Code VII Division 1. VIII. New York: The American Society of Mechanical Engineers, (2007).